

Copyright © 1983, by the author(s).
All rights reserved.

Permission to make digital or hard copies of all or part of this work for personal or classroom use is granted without fee provided that copies are not made or distributed for profit or commercial advantage and that copies bear this notice and the full citation on the first page. To copy otherwise, to republish, to post on servers or to redistribute to lists, requires prior specific permission.

POTENTIAL BARRIER DECOUPLING OF STABLE AND UNSTABLE
REGIONS OF AVERAGE-MINIMUM-B MAGNETIC MIRRORS

by

J.C. Fernandez, A.J. Lichtenberg, M.A. Lieberman and N.M.P. Benjamin

Memorandum No. UCB/ERL M83/22

26 January 1983

ELECTRONICS RESEARCH LABORATORY

College of Engineering
University of California, Berkeley
94720

POTENTIAL BARRIER DECOUPLING OF STABLE AND UNSTABLE
REGIONS OF AVERAGE-MINIMUM-B MAGNETIC MIRRORS

J.C. Fernandez, A.J. Lichtenberg, M.A. Lieberman, and N.M.P. Benjamin

Department of Electrical Engineering and Computer Sciences
and the Electronics Research Laboratory
University of California, Berkeley, California 94720

ABSTRACT

A mirror-confined hot-electron distribution is created in a single magnetically stable cell of a multiple mirror device. The hot electrons are observed to decouple magnetically stable and unstable portions of the plasma on the two sides of the cell containing the hot electrons. The unstable motion is found to be flute-like with velocity comparable to that expected from the unstable portion by itself. The plasma partially restabilizes later in time. The decoupling is interpreted as caused by a potential barrier created in the ECRH mirror cell. The coupling is restored with the decay of the potential barrier as ions become trapped in the cell.

One of the most promising configurations being investigated for confinement of fusion plasmas is that of a tandem mirror in which a potential barrier to electron flow is formed between regions of unstable and stable magnetic curvature [1]. In the absence of the barrier the entire pressure weighted curvature is stable. This configuration has been analyzed using drift-kinetic equations [2] to study trapped particle modes. The result is that the plasma is unstable if the density is sufficiently small in the potential barrier region, an approximate stability criterion being (for the lowest order $m = 1$ azimuthal mode)

$$\frac{n_s}{n_0} > 4 \frac{r_p}{R} \quad (1)$$

where n_s/n_0 is the ratio of the transition or sheath density (which samples both the stable and unstable curvature regions) to the unstable plasma density, and r_p/R is the ratio of plasma radius to the average unfavorable radius of curvature. Equation (1) implies that the usual tandem mirror configuration would be unstable for a fully developed plasma sheath, in which $n_s/n_0 \approx (m_e/m_i)^{1/2}$ to preserve the Boltzmann distribution of electrons [$(m_e/m_i)^{1/2} \approx 1/40$, for hydrogen]. Theoretically, it should be possible to tailor the machine design such that the potential barrier serves its confinement function without producing this trapped particle instability [3].

A curvature driven resistive trapped particle instability is also expected to be present in tokamaks, where the prediction is that high mode numbers are unstable, leading to plasma turbulence [4]. Although turbulence is commonly seen in tokamaks, under conditions in which the trapped particle mode should exist, positive identification has not been possible. More recently, a direct observation of the trapped ion

mode has been made in its collisional form [5].

Unlike the above experiments, in the tandem mirror configuration the mode is expected to be mainly flute-like, in which the most dangerous mode is probably $m=1$, with corresponding transverse plasma flow to the walls. A flute-like mode corresponds to early experiments in which a mirror-confined plasma with MHD unstable curvature was terminated, outside of the mirrors, on conducting plates. The effect of the end-plates on stability in these experiments was not fully understood. If the plates were not emitting, various experiments reported stabilization [6], destabilization [7], or no effect at all [8]. An emitting end plate with an electron-rich sheath is stabilizing, with a transition to instability as the sheath becomes ion rich [9]. An interpretation of these results can be given in terms of the resistive nature of the normal sheath existing between a plasma and either a non-emitting conductor or an ion-rich sheath [10,7,11]. The combined system is then always unstable, but at reduced growth rates, which may or may not be observed in a given experiment. A general consensus, however, is that a passive conducting end plate cannot be used to stabilize a mirror-confined plasma at fusion parameters [11].

It is the purpose of the present note to describe experimental observations of instabilities in tandem-mirror-like magnetic configurations in which MHD modes localized in unfavorable curvature regions have been produced.

In the experiment, shown in Fig. 1, plasma is injected into one end of a multiple-mirror device [12] through a rising cusp field. The plasma then flows into a quadrupole stabilized cell in which the electron cyclotron resonance heating (ECRH) is performed, and into a set of unstable cells. The metal chamber walls of the ECRH cell, together with

end plates with openings shaped to fit the elliptical finx surfaces, form a cavity for ECRH which does not obstruct the stable plasma flow.

Without ECRH the entire plasma is avg-min-B stable through most of its decay, due to the strong stabilizing effect of the cusp. (late in the decay an MHD flute instability develops when the cusp is sufficiently emptied of plasma.)

When a 10 GHZ ECRH heating pulse ($\sim 200\text{kW}$, $3 \mu\text{sec}$) is injected into the quadrupole-stabilized mirror cell at an appropriate plasma density ($\omega_p \lesssim \omega_{rf}$) a mirror-trapped hot electron distribution is established in the ECRH cell, as evidenced by the production of x-rays. The temperature of the electron distribution was measured from x-ray pulse height analysis to be approximately 1 keV. The hot electrons decayed with a time constant of about 1 msec, characteristic of Coulomb collisional processes.

A direct measurement of the potential in the ECRH cell has not been made. Theoretically, we expect a negative potential to be formed because, by charge neutrality, the cold electron density in the ECRH cell is reduced below its value in the adjacent cells. The Boltzmann condition on the cold electrons (having temperature T_c) then requires the existence of a potential barrier. If all the electrons in the cell are heated then we would expect that the Boltzmann condition would force a negative potential of approximately $4T_c$ to exist in that cell, reducing the cold electron density to that existing in a typical sheath.

Two indirect measurements indicate that a potential has been formed. In the first, with an avg-min-B stable magnetic field configuration, the ion saturation current on a Langmuir probe in the adjacent up-stream (high density) mirror cell is found to increase within 10 μsec after heating, while the ion saturation current on a Langmuir probe in the down-stream (lower density) cell is found to decrease with roughly

the same time constant. On a longer time scale ($\sim 50 \mu\text{sec}$) these transients disappear. These observations are qualitatively interpreted as arising, at least in part, from a perturbation in the plasma flow due to the formation of a potential barrier. The potential decays on the time scale for ions to collisionally become trapped in the ECRH cell. A second indication of this barrier is obtained using an 8 mm fixed-frequency interferometer. The interferometer measurements indicate an increase in the plasma density in the ECRH cell on a time scale of $50 \mu\text{sec}$ after heating. This density increase is predicted to occur by the same mechanism that destroys the potential barrier, that is, by collisional trapping of ions within the ECRH cell.

With a magnetic field such as that shown in Fig. 1, the ECRH-produced hot electrons are found to decouple the colder plasma in the two portions of the machine on each side of the ECRH cell. Since only plasma on one side of the ECRH cell is cusp stabilized, the result of the decoupling is that the other side of the machine becomes unstable. The large amplitude motion leads to significant plasma loss. This is shown, for one particular set of parameters, in Fig. 2, using on-axis Langmuir probes operating in the ion saturation region. At the time of heating (arrow) the characteristic transient increase in ion saturation current is seen on the upstream probe at midplane M_{78} . There is a corresponding rapid loss of plasma on the axis of the downstream midplane M_{56} . The x-ray production at the midplane M_{67} of the ECRH cell is also shown. The characteristic decay time of the x-rays is that predicted for the scattering of 1 keV electrons into the loss cone, and is independent of the decay of the cooler plasma.

The time for the decay of the potential barrier by ion trapping is expected to be approximately 50 μsec . On this time scale we would expect plasma reconnection to be established. However, reconnection with an off-center plasma can be impeded by the end plates of the ECRH cavity. A set of four off-axis Langmuir probes are used to view the resultant plasma motion. An analysis of typical shots indicates primarily an $m=1$ mode with some admixture of $m=2$. Depending on the shot, varying amounts of plasma may be lost before a partial reconnection is established. A rather different type of behavior, in which the plasma in the unstable field region has wide excursions but is not lost, is illustrated in Fig. 3. Rather than showing the probe traces directly, we plot the centroid of the plasma motion each 5 μsec as determined from the four off-axis probes. Early in time, $25 \mu\text{s} < t < 35 \mu\text{sec}$, the motion of the centroid is rapid, as expected from the ExB motion of the fully developed instability. Later in time, $105 \mu\text{s} < t < 115 \mu\text{sec}$ large amplitude motion persists, but the velocity has been considerably reduced. We interpret this as indicating at least partial restabilization of the plasma. The complicated trajectory of the centroid indicates that the wall is playing a significant role in the motion for the off-center plasma. The initial off-center position of the plasma (at $t=0$) when the ECRH is employed allows the instability to develop rapidly. Noise on the probes prevented measurements during the first 25 μsec after ECRH.

Experiments were also performed by injecting a plasma from a θ -pinch source through a cusp on the left end of the device. With this configuration the field in the cell to the right of the ECRH cell (see Fig. 1) was changed from a cusp to that of an unstable mirror. After firing the ECRH, the two parts of the device again decoupled with large

amplitude oscillations and plasma loss observed to the right of the ECRH cell, while the left side, including the cusp, although showing some motion, remained essentially stable.

To compare our results with theory we use either the approximate dispersion relation from the drift-kinetic analysis or the dispersion relation employing a resistive sheath. From the drift-kinetic analysis the dispersion relation is (1)

$$\omega^2 \left(\frac{n_s}{n_0} + k_{\perp}^2 \rho_i^2 \right) - \omega \omega_* \left(\frac{n_s}{n_0} + k_{\perp}^2 \rho_i^2 \right) + \omega_* \omega_c = 0 \quad (2)$$

where $\omega_* = \frac{T}{eBr_p} \left(\frac{1}{n} \frac{dn}{dr} \right)$ is the diamagnetic drift frequency $\omega_c = k_{\perp} \frac{T}{eB R}$ is the magnetic curvature drift frequency ($R = L_B/r_p$ being the magnetic curvature with L_B the magnetic scale length), ρ_i is the ion gyroradius, and the other symbols have their usual meaning (with T in volts).

Putting $k_{\perp} = 1/r_p$ ($m=1$ mode) then for $n_s/n_0 \gg (\rho_i/r_p)$, we obtain Eq. (1).

For our parameters, $2 < r_p < 3$ cm, $L_B = 30$ cm, $T_e = T_i \approx 5$ eV, the plasma is unstable, according to Eq. (1), if all of the electrons are heated ($\frac{n_s}{n_p} \approx \frac{1}{40}$). The growth time, according to (2) has a maximum of $\tau_g \approx 80$ μ sec for $r_p \approx 3$ cm, which is about a factor of six larger than the flute growth time $\tau_f \approx L_B/v_{T_i} \approx 13$ μ sec.

The instability growth time can also be estimated from the resistive sheath model with the reduction in the growth rate for the $m=1$ mode obtained approximately as [11]

$$\frac{\tau_g}{\tau_f} \approx \frac{1}{\sqrt{2\pi}} \frac{r_p^2}{\rho_i^2} \cdot \frac{L_B}{L_p} \left(\frac{T_i}{T_e} \right)^2 \left(1 + \frac{T_e}{T_i} \right)^{-1/2} \quad (3)$$

where L_p is the length of the unstable plasma. As in the trapped particle mode analysis, the stable region is considered to be a region of zero mode amplitude, i.e., act like a conducting wall. Using the previous parameters (but taking $r_p = 2\text{cm}$ at the lower end of the range to minimize τ_g) and with $L_p = 3$ meters we find $\tau_g/\tau_f \approx 7$ or $\tau_g \approx 90 \mu\text{sec}$. In the resistive sheath model there is no sharp transition with n_s/n_0 between stable and unstable behavior.

For either analysis the calculated growth time is considerably slower than the time for the large amplitude motion to move the plasma a distance equal to its radial extent. We note that there is a fairly large initial perturbation which permits a fully developed initial motion, rather than requiring an initial time for exponentiation. However, even allowing for this the motion is more rapid than expected. One possible explanation might be transient heating of the electrons resulting from the r.f. leakage fields.

A second difficulty is that a nearly full sheath potential is required to keep n_s/n_0 sufficiently small that Eq. (1) predicts instability. Although the resistive sheath model predicts instability for larger n_s/n_0 , the growth rate rapidly falls off as n_s/n_0 increases. In addition to the decay of the potential expected from ion trapping, other effects may prevent a full sheath potential from building up (or maintain n_s/n_0 at a larger value). Variation in n_s/n_0 may be responsible for the wide variation of the shot-to-shot behavior, as would be predicted from Eq. (2).

On a longer time scale the cusp tends to empty, and the entire colder plasma may become flute unstable, independent of the hot-electron component which remains stable. The existence of a hot-electron component, together with overall charge neutrality, leads to a charge

imbalance between the colder electron and ion components. This charge imbalance has been predicted to be stabilizing [13,14]. However, the percentage of hot electrons late in time (estimated to be 5% of the total number of electrons in the 8 cell multiple mirror device) is not known accurately and may be too small to achieve stability.

We also note that the decoupling of the hot-electron and colder components has been confirmed by modifying the ECRH cell magnetic fields such that the hot-electron component is not fully stabilized. The hot electrons can then be made to dump independently of the colder plasma, which remains cusp stabilized.

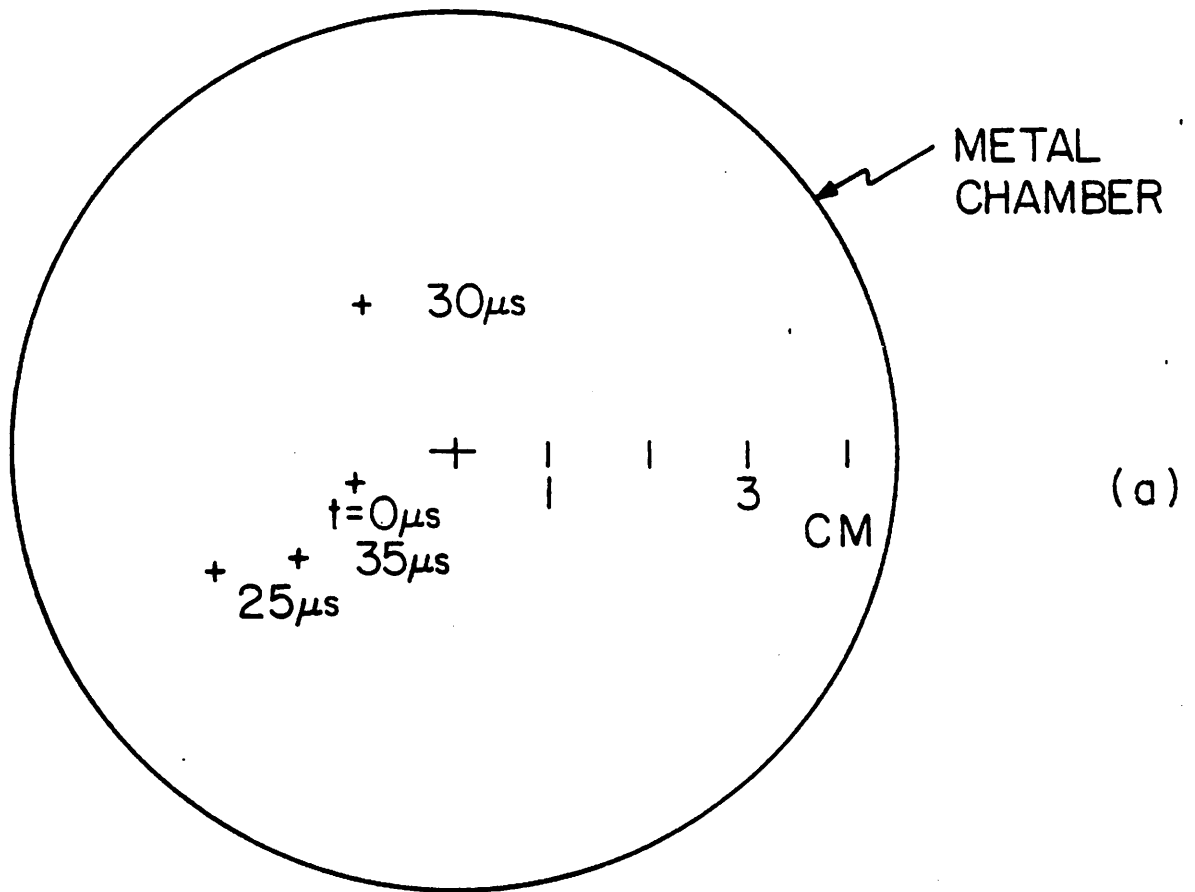
In conclusion, the decoupling of stable and unstable magnetic field regions of an average-minimum-B device, by the creation of an intervening hot-electron distribution, has been experimentally demonstrated. Theoretical calculations from either a trapped particle or a resistive sheath model predict the behavior qualitatively, but not quantitatively. A time resolved measurement of the potential in the barrier region will be required to more clearly delineate the decoupling mechanism.

The work was supported by DOE Contract DE-AT03-76ET53059 and NSF Grant ECS 8104561.

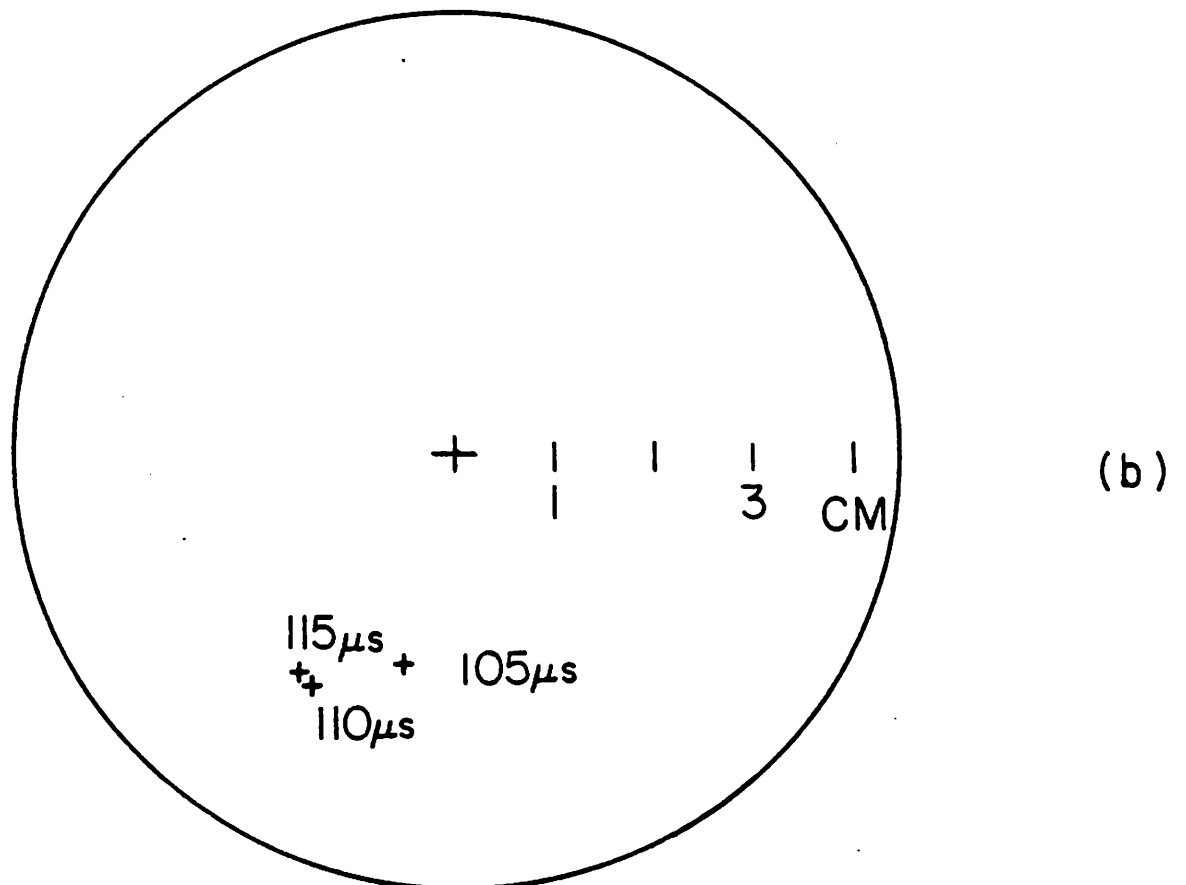
REFERENCES

- [1] D.E. Baldwin and B.G. Logan, Phys. Rev. Lett., 43, 1318 (1979).
- [2] T.M. Antonsen, D.E. Baldwin, H.L. Berk, M.N. Rosenbluth, and H.V. Wong, Soviet J. of Plasma Phys., to be published; see also M.N. Rosenbluth, "Topics in Plasma Instabilities: Trapped-Particle Modes and MHD," Int. Plasma Physics Conf., Goteborg, Sweden, June 1982.
- [3] "Physics Basis for an Axicell Design for the End Plugs of MFTF-B," D.E. Baldwin and B.G. Logan, Ed., Lawrence Livermore Laboratory, UCID 19359, April 1982.
- [4] B.B. Kadomtsev and O.P. Pogutse, Nucl. Fusion, 11, 67 (1971).
- [5] D.P. Dixon, A.K. Sen, and T.C. Marshall, Plasma Phys., 20, 253 (1978).
- [6] F.H. Coensgen, W.F. Cummins, W.E. Nexsen, and A.E. Sherman, Phys. Fluids, 9, 186 (1966).
- [7] R. Prater, Phys. Fluids, 17, 193 (1974).
- [8] I.A. Brown, A.J. Lichtenberg, M.A. Lieberman, and N. Convers Wyeth, Phys. Fluids, 19, 1203 (1976).
- [9] F.F. Chen, Phys. Fluids, 8, 752 (1965).
- [10] W.B. Kunkel and J.W. Guillery, in Proc. of the Seventh Int. Conf. on Phenomenon in Ionized Cases, Belgrade, Vol. II, 707 (1966).
- [11] M.A. Lieberman and S.L. Wong, Plasma Phys., 19, 745 (1977).
- [12] M. Tuszewski, D. Price, M.A. Lieberman, R. Bravenec, K. Doniger, C. Hartman, and A.J. Lichtenberg, Nucl. Fusion, 19, 1244 (1979).
- [13] A.J. Lichtenberg and M.A. Lieberman, Evaluation of ECRH Experiments in MMX, Unpublished Report, Dec. 1980.
- [14] J. Kesner, R.S. Post, D.K. Smith, and D.E. Baldwin, Nuclear Fusion, 22, 577 (1982).

Fig. 3. Motion of the centroid (pluses) of the plasma density cross-section with time:



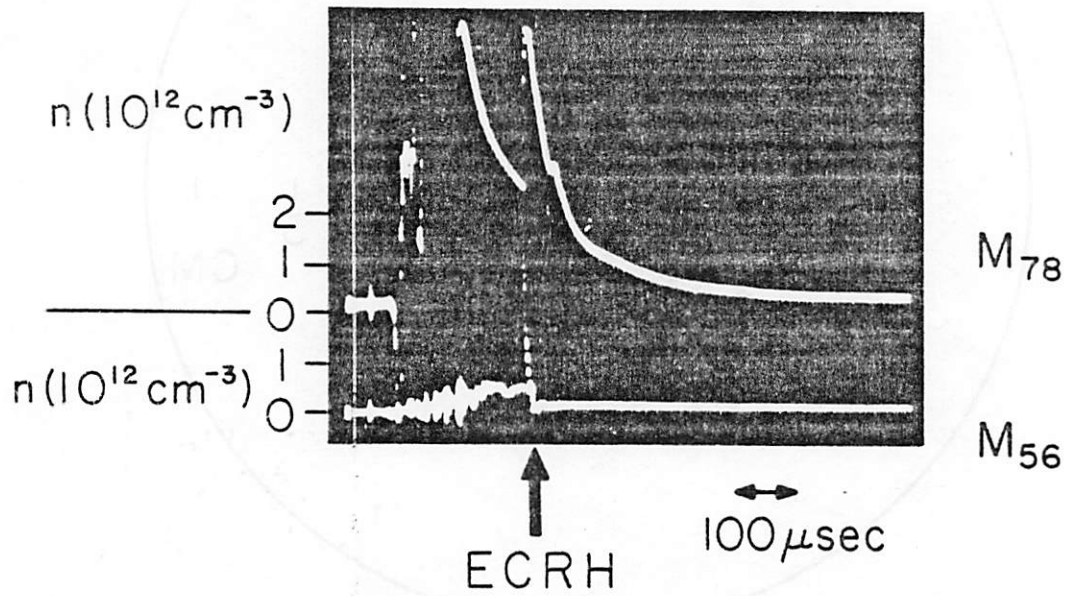
(a) early in time;



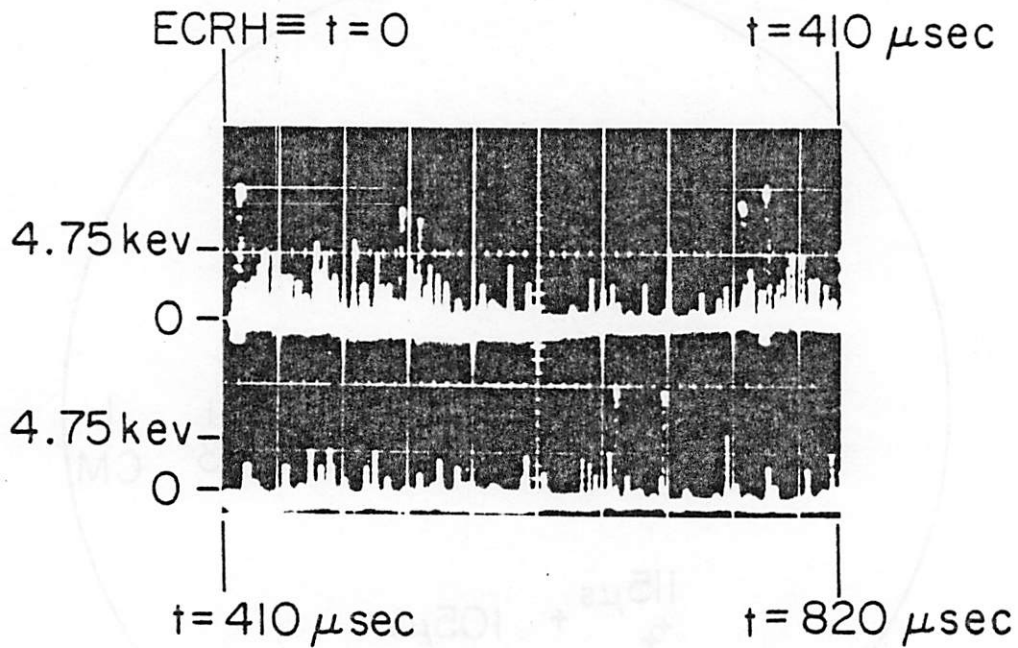
(b) later in time. Time $t = 0$ corresponds to the ECRH heating time.

Fig. 2. (a) The density decay on axis at the midplane of the stable cell (M_{78}) and at the midplane of a cell that becomes unstable after ECRH (M_{56}).

(b) Single x-rays emitted perpendicular to the midplane of the ECRH cell (M_{67}); note the two traces are two halves (in time) of a single record.



(a)



(b)

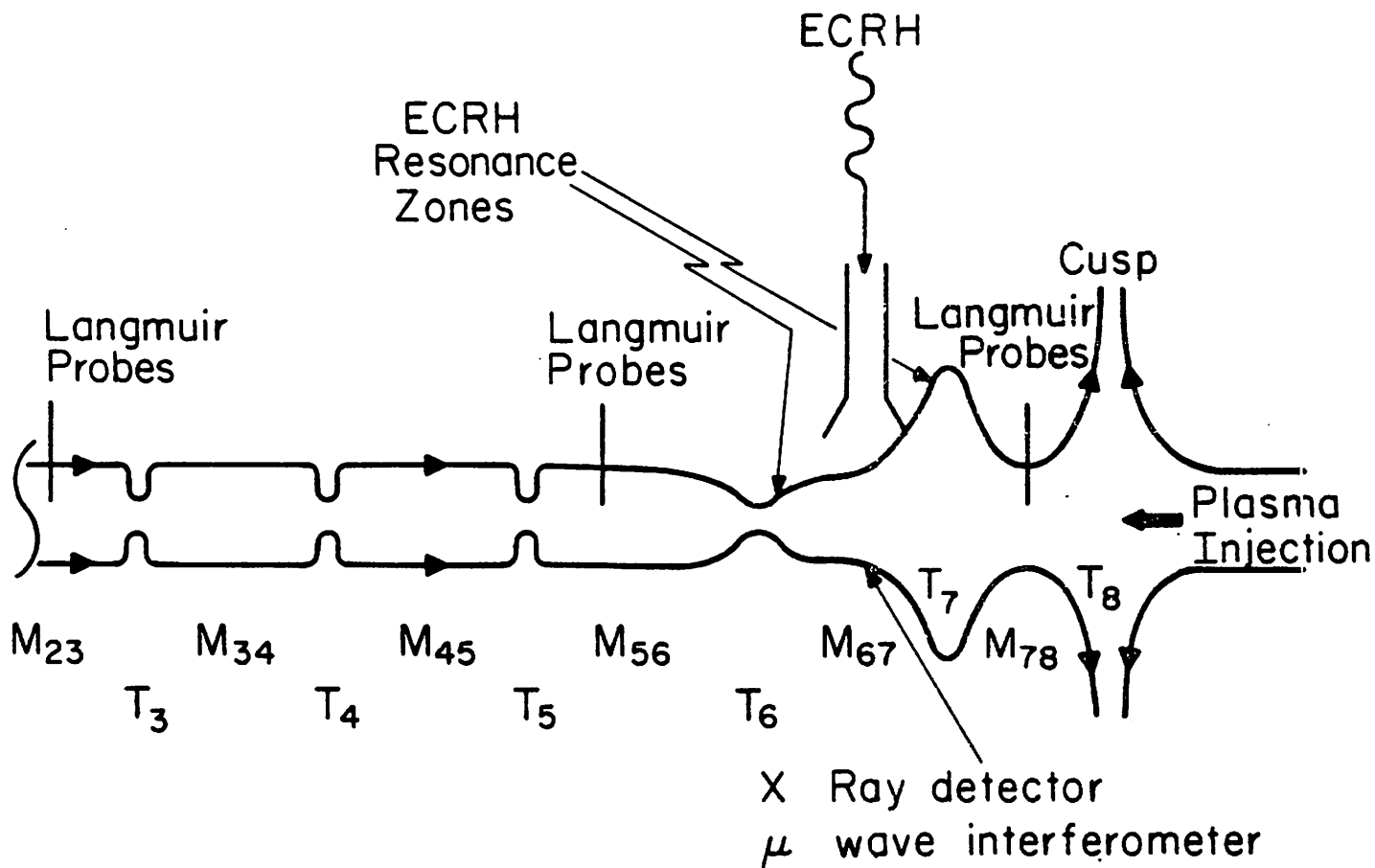


Fig. 1. Schematic (not to scale) of two field lines 180° apart in the multiple mirror device showing midplanes (M) mirror throats (T) and the position of the ECRH and various diagnostics.